

Three-Dimensional Computational Fluid Dynamics Models of Heat Distribution in Autoclave Reactors for Ethylene Polymerization

Suchanan Mekchai, Thanyalak Jaherng, Teerawat Sema and Pornchai Bumroongsri*

Department of Chemical Engineering, Faculty of Engineering, Mahidol University, Thailand

*Corresponding author, e-mail: pornchai.bum@mahidol.ac.th

Abstract

Computational Fluid Dynamics (CFD) is one of the most useful computational methods that are widely used to predict the fluid behavior in many industrial processes including low-density polyethylene (LDPE) production process in an autoclave reactor. In this paper, a CFD model of autoclave polymerization reactors for LDPE production is developed. Polymerization initiator is premixed with ethylene monomer and the mixture is then fed to the reactor. The product leaves the reactor at the outlet pipe. There are two main reactions in this process which are the polymerization and decomposition of ethylene. Decomposition reaction can produce a large amount of heat and be able to cause runaway phenomena. The developed CFD model can predict the distribution of temperature profiles. The effects of the inlet initiator mass fraction and the inlet temperature are studied. The runaway phenomena can be reduced by a proper adjusting of the inlet initiator mass fraction and the inlet temperature. From the simulation results, the highest inlet initiator mass fraction and inlet temperature that can prevent the runaway phenomena are 1.2×10^{-4} and 460 K, respectively.

Keywords: *computational fluid dynamics, autoclave polymerization reactor, low-density polyethylene, temperature distribution, decomposition of ethylene*

1. Introduction

Polyethylene (PE) is a thermoplastic that has been commonly used worldwide. Low-density polyethylene (LDPE), which is one of the PE families, has been found to be used in various applications such as plastic bags, insulations, and coatings. LDPE was first produced in 1993 by Imperial Chemical Industries (ICI) through a high pressure process via free radical polymerization. At present, the demand of LDPE is found to be high in Asia, especially in Thailand, due to its various useful applications.

In the autoclave polymerization reactor, the ethylene monomer is reacted at very high pressure along with the initiator. Peroxide has been considered as one of the mostly use initiator. At high temperature, it can be decomposed into free radical which can react rapidly with the ethylene monomer to create longer radical chains. These chains then combine with each other to polymer chains known as polymerization reaction. In accordance with the polymerization reaction, the ethylene monomer can also be decomposed in the autoclave reactor. Thus, there are two main reactions taking place in the autoclave reactor including the polymerization and the decomposition of ethylene. The polymerization reaction of ethylene is highly exothermic and occurs at high pressure (1,000 to 3,000 atm) and high temperature (140 to 330°C). According to a polyethylene production, the polymerization of ethylene is considered as a desired reaction as shown in Table 1. The polymerization kinetics can be obtained from Zhou, Marshall and Oshinowo (2001) where I is the initiator, M is the monomer, A is the initiator radical, R_x and R_y are the live polymer with chain length x and y , respectively, and, P_x and P_y are the dead polymer with chain length x and y , respectively.

Table 1 Polymerization reaction

Type	Reaction
Initiator decomposition	$I \xrightarrow{k_I} 2A$
Chain initiation	$A + M \xrightarrow{k_{II}} R_1$
Chain propagation	$R_x + M \xrightarrow{k_p} R_{x+1}$
Chain transfer to monomer	$R_x + M \xrightarrow{k_{tm}} P_x + R_1$
Disproportionation termination	$R_x + R_y \xrightarrow{k_{dt}} P_x + P_y$
Combination termination	$R_x + R_y \xrightarrow{k_c} P_{x+y}$

At high temperature and high pressure of polyethylene production, the runaway reaction, which is the decomposition of ethylene monomer, can occur in the process. In the decomposition of ethylene, ethylene is decomposed into various products such as carbon (C), methane (CH_4), hydrogen (H), acetylene (C_2H_2), ethane (C_2H_6) and hydrocarbons as shown in Table 2. The dot symbol (\bullet) represents the intermediate of respective substance. A large amount of heat is then found to be produced in accordance with the decomposition of ethylene (Zhang, Read, & Ray, 1996; Villa, Dihora, & Ray, 1998; Kolhapure, Fox, Daiss, & Mahling, 2005). The phenomena occur in a very small time interval and can lead to the runaway phenomena. Therefore, a well understood of the behavior in the autoclave polymerization reactor is necessary to avoid the runaway phenomena.

Table 2 Decomposition reaction

Type	Reaction
Initiation	$2M \xrightarrow{k_1} C_2H_3^\bullet + C_2H_5^\bullet$
Propagation	$C_2H_5^\bullet \xrightleftharpoons[k_2, k_2']{k_2} M + H^\bullet$
Propagation	$C_2H_5^\bullet + M \xrightarrow{k_3} C_2H_6 + C_2H_3^\bullet$
Propagation	$H^\bullet + M \xrightarrow{k_4} H_2 + C_2H_3^\bullet$
Propagation	$C_2H_3^\bullet \xrightarrow{k_5} C^S + CH_3^\bullet$
Propagation	$CH_3^\bullet + M \xrightarrow{k_6} CH_4 + C_2H_3^\bullet$
Termination	$2CH_3^\bullet \xrightarrow{k_7} C_2H_6$
Termination	$CH_3^\bullet + C_2H_3^\bullet \xrightarrow{k_8} CH_4 + C_2H_2$
Termination	$2C_2H_3^\bullet \xrightarrow{k_9} C_2H_2 + M$

Computational fluid dynamics (CFD) is a powerful computational tool that is popularly used in the prediction of flow behavior. Although several publications on the mathematical simulations of LDPE autoclave reactors have been published (Ham & Rhee, 1996; Read, Zhang, & Ray, 1997; Tosun & Bakker, 1997; Pladis & Kiparissides, 1999; Zhou et al., 2001; Zheng et al., 2014), these papers considered only the polymerization reaction, while the decomposition reactions was usually omitted in the CFD modeling and simulation.

In this paper, a 3D CFD modeling of the autoclave polymerization reactor for LDPE production is developed in Fluent 16.0. The novelty is that both polymerization and decomposition reactions are taken into account. The developed CFD model is then used to study the effects of operating parameters including the initiator mass fraction and the inlet temperature on the temperature distribution. The heat transfer phenomena are studied to avoid the runaway reaction from ethylene decomposition.

2. Objectives

1. To develop the 3D CFD model of autoclave reactor for ethylene polymerization.
2. To study the effects of the inlet initiator mass fraction and the inlet temperature on the temperature distribution.

3. Material and Methods

3.1 CFD model development of autoclave polymerization reactor

There are several steps in the CFD model development of autoclave polymerization reactor as follows. The kinetic parameters for polymerization reactions are obtained from Zhou et al. (2001). The kinetic parameters for decomposition reactions are obtained from Zhang et al. (1996).

3.2 Setting up the geometry and transport equations

(1) Creating geometry

The autoclave reactor is a stirred-tank reactor that consists of multiple zones. The reactor in this paper is constructed based on the one described by Zhou et al. (2001). The specifications of autoclave reactor are listed in Table 3. The initiator which is Di-tert-butyl peroxide (DTBP) is premixed with the ethylene monomer at the reactor inlet. The mixture enters the reactor and the product leaves the reactor at the outlet.

Table 3 Physical specifications of autoclave reactor

Physical Specifications	Values	Units
Volume of reactor	498	L
Height of reactor	1.59	m
Diameter of reactor	0.64	m
Inlet and outlet pipe diameters	0.02	m
Impeller diameter	0.40	m
Impeller height	0.08	m
Impeller width	0.02	m
Diameter of the shaft	0.20	m
Number of paddles	4	-

(2) Generating mesh

The 3D geometry of LDPE autoclave reactor is represented in Figure 1(a). The 3D geometry can be partitioned into 115,117 cells as shown in Figure 1(b).

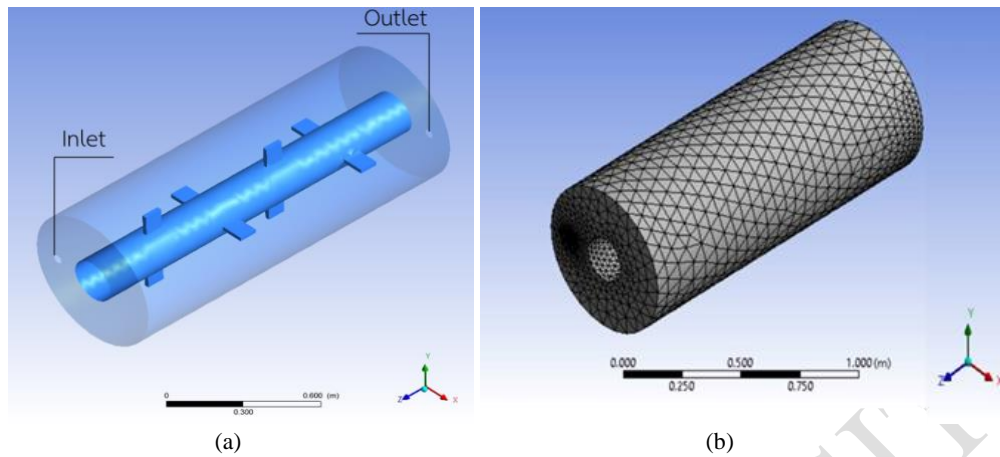


Figure 1 Autoclave reactor (a) geometry and (b) mesh

(3) Setting up the data and transport equations

The transport equations are included in the CFD model. They consist of the species, momentum and energy transport equations as shown in equation (1)-(3), respectively.

$$\frac{\partial}{\partial t}(\rho Y_i) + \nabla \cdot (\rho \vec{v} Y_i) = -\nabla \cdot \vec{J}_i + S_i \quad (1)$$

$$\frac{\partial}{\partial t}(\rho \vec{v}) + \nabla \cdot (\rho \vec{v} \vec{v}) = -\nabla p + \nabla \cdot (\vec{\tau}) + \rho \vec{g} + F \quad (2)$$

$$\rho C_p \frac{\partial T}{\partial t} + \rho C_p \vec{v} \cdot \nabla T = \nabla \cdot (k \nabla T) + Q \quad (3)$$

Where i denotes the species number, Y_i is the mass fraction, S_i is the rate of creation by addition (source term), \vec{J}_i is the diffusion flux, ρ is the density, \vec{v} is the velocity, p is the pressure, $\vec{\tau}$ is the stress tensor, \vec{g} is the gravitational acceleration, F is the force term, C_p is the heat capacity, T is temperature, k is thermal conductivity and Q is the heat source. The operating parameters of autoclave reactor are listed in Table 4.

Table 4 Operating parameters

Name	Value	Units
Impeller speed	250	rpm
Inlet mass flow rate of mixture	8	kg/s
Viscosity of mixture	1.6×10^{-3}	kg/(m·s)
Density of mixture	499	kg/m ³
Impeller speed	250	rpm
Inlet mass flow rate of mixture	8	kg/s

3.3 Including the kinetic reactions of LDPE polymerization in CFD model

The source terms of the polymerization reactions can be written in Table 5.

Table 5 The source terms for polymerization reactions.

$S_I = -k_I[I]$
$S_A = 2k_I[I] - k_{II}[A][M]$
$S_M = -k_{II}[A][M] - k_p[M] \sum_{x=1}^{\infty} R_x - k_{trm}[M] \sum_{x=1}^{\infty} R_x$
$S_{R_x} = k_p[M]R_x + k_p[M]R_{x-1} - (k_{tc} + k_{td})R_x \sum_{y=1}^{\infty} R_y + \delta(x-1)k_{II}[A][M] - k_{trm}[M]R_x + \sum_{x=1}^{\infty} k_{trm}\delta(x-1)[M]R_y$
$S_{P_x} = k_{td}R_x \sum_{x=1}^{\infty} R_y + \frac{1}{2}k_{tc} \sum_{x=1}^{\infty} R_{x-y}R_y + k_{trm}[M]R_x$

Where $\delta(x-1)=1$ when $x=1$ and $\delta(x-1)=0$ when $x \neq 1$. Due to the fact that the chain length x and y can have many values, it is impossible to write the species balance for each chain length. In this paper, the method of moments is applied to reduce the number of equations. The moments of live polymer (λ) and dead polymer (μ) are defined as

$$\lambda_0 = \sum_{x=1}^{\infty} R_x, \quad \lambda_1 = \sum_{x=1}^{\infty} xR_x, \quad \lambda_2 = \sum_{x=1}^{\infty} x^2 R_x \quad (4)$$

$$\mu_0 = \sum_{x=1}^{\infty} P_x, \quad \mu_1 = \sum_{x=1}^{\infty} xP_x, \quad \mu_2 = \sum_{x=1}^{\infty} x^2 P_x \quad (5)$$

Where $\lambda_0, \lambda_1, \lambda_2$ are the 0th, 1st, 2nd moments of live polymer, respectively, and μ_0, μ_1, μ_2 are the 0th, 1st, 2nd moments of dead polymer, respectively. By multiplying each source term for polymerization reactions in Table 5 by x^n (where n is either 0, 1, or 2) and summing the resulting expressions over the total range of variation of x , the revised set of source terms can be written in Table 6.

Table 6 The revised set of source terms

$S_I = -k_I[I]$
$S_A = 2k_I[I] - k_{II}[A][M]$
$S_M = -k_I[A][M] - k_p\lambda_0[M] - k_{trm}\lambda_0[M]$
$S_{\lambda_0} = S_R = -(k_{td} + k_{tc})\lambda_0^2 + k_{II}[A][M]$
$S_{\lambda_1} = -(k_{td} + k_{tc})\lambda_0\lambda_1 + k_{II}[A][M] + k_p\lambda_0[M] + k_{trm}[M](\lambda_0 - \lambda_1)$
$S_{\lambda_2} = -(k_{td} + k_{tc})\lambda_0\lambda_2 + k_{II}[A][M] - k_p\lambda_0[M] + 2k_p\lambda_1[M] + k_{trm}[M](\lambda_0 - \lambda_2)$
$S_{\mu_0} = S_P = (k_{td} + \frac{1}{2}k_{tc})\lambda_0^2 + k_{trm}\lambda_0[M]$
$S_{\mu_1} = (k_{td} + k_{tc})\lambda_0\lambda_1 + k_{trm}\lambda_1[M]$
$S_{\mu_2} = (k_{td} + k_{tc})\lambda_0\lambda_2 + k_{tc}\lambda_1^2 + k_{trm}\lambda_2[M]$
$S_{T_{poly}} = -\Delta H(-k_I[A][M] - k_p\lambda_0[M] + k_{trm}\lambda_0[M])$

The ethylene decomposition reactions are included to the developed CFD model due to the fact that the thermal runaway is a problem in LDPE autoclave reactor plant. Therefore, the decomposition reactions are added into the developed CFD model in order to study the phenomena of runaway within autoclave reactor. The decomposition reactions of ethylene obtained from Zhang et al. (1996) are shown in Table 2, the source terms of these transport equations are shown in Table 7.

Table 7 The source terms for ethylene decomposition kinetics

$S_M = -2k_1[M]^2 + k_2[C_2H_5^\bullet] - k_2'[M][H^\bullet] - k_3[C_2H_5^\bullet][M]$ $- k_4[H^\bullet][M] - k_6[CH_3^\bullet][M] + k_t[C_2H_3^\bullet]^2$
$S_{C_2H_5^\bullet} = k_1[M]^2 - k_2[C_2H_5^\bullet] + k_2'[M][H^\bullet] - k_3[C_2H_5^\bullet][M]$
$S_{H^\bullet} = k_2[C_2H_5^\bullet] - k_2'[M][H^\bullet] - k_4[H^\bullet][M]$
$S_{C_2H_3^\bullet} = k_1[M]^2 + k_3[C_2H_5^\bullet][M] + k_4[H^\bullet][M] - k_5[C_2H_3^\bullet]$ $+ k_6[CH_3^\bullet][M] - k_t[C_2H_3^\bullet][CH_3^\bullet] - k_t[C_2H_3^\bullet]^2$
$S_{C_2H_6} = k_3[M][C_2H_5^\bullet] + k_t[CH_3^\bullet]^2$
$S_{H_2} = k_4[H^\bullet][M]$
$S_C = k_5[C_2H_3^\bullet]$
$S_{CH_3^\bullet} = k_5[C_2H_3^\bullet] - k_6[CH_3^\bullet][M] - k_t[CH_3^\bullet]^2 - k_t[C_2H_3^\bullet][CH_3^\bullet]$
$S_{CH_4} = k_6[CH_3^\bullet][M] + k_t[C_2H_3^\bullet][CH_3^\bullet]$
$S_{C_2H_2} = k_t[C_2H_3^\bullet][CH_3^\bullet] + k_t[C_2H_3^\bullet]^2$
$S_{T_{decomp}} = -\Delta H_{decomp} \left(3k_1 + k_6 \sqrt{\frac{2k_1}{k_t}} \right) [M]^2$

By substituting the concentration of radicals, the source terms for ethylene decomposition can be summarized as

$$S_C = k_5[C_2H_3^\bullet] = \frac{k_6}{2} \sqrt{\frac{2k_1}{k_t}} [M]^2 \quad (6)$$

$$S_{CH_4} = k_6[M][CH_3^\bullet] + k_t[C_2H_3^\bullet][CH_3^\bullet] = \left(\frac{k_1}{2} + \frac{k_6}{2} \sqrt{\frac{2k_1}{k_t}} [M]^2 \right) \quad (7)$$

$$S_{C_2H_6} = k_3[M][C_2H_5^\bullet] + k_t[CH_3^\bullet]^2 = \frac{3}{2} k_1 [M]^2 \quad (8)$$

$$S_{C_2H_2} = k_t[C_2H_3^\bullet][CH_3^\bullet] + k_t[C_2H_3^\bullet]^2 = k_1 [M]^2 \quad (9)$$

The final expressions for the chemical source terms are shown in Table 8. All source terms are written as the UDF files to incorporate into the CFD modeling.

Table 8 Final expressions for all source terms

$S_I = -k_I[I]$
$S_A = 2k_I[I] - k_{II}[A][M]$
$S_{\lambda_0} = -(k_{td} + k_{tc})\lambda_0^2 + k_{II}[A][M]$
$S_{\lambda_1} = -(k_{td} + k_{tc})\lambda_0\lambda_1 + k_{II}[A][M] + k_p\lambda_0[M] + k_{trm}[M](\lambda_0 - \lambda_1)$
$S_{\lambda_2} = -(k_{td} + k_{tc})\lambda_0\lambda_2 + k_{II}[A][M] - k_p\lambda_0[M] + 2k_p\lambda_1[M] + k_{trm}[M](\lambda_0 - \lambda_2)$
$S_{\mu_0} = \left(k_{td} + \frac{1}{2}k_{tc}\right)\lambda_0^2 + k_{trm}\lambda_0[M]$
$S_{\mu_1} = (k_{td} + k_{tc})\lambda_0\lambda_1 + k_{trm}\lambda_1[M]$
$S_{\mu_2} = (k_{td} + k_{tc})\lambda_0\lambda_2 + k_{tc}\lambda_1^2 + k_{trm}\lambda_2[M]$
$S_C = \frac{k_6}{2} \sqrt{\frac{2k_1}{k_1}} [M]^2$
$S_{CH_4} = \left(\frac{k_1}{2} + \frac{k_6}{2} \sqrt{\frac{2k_1}{k_1}}\right) [M]^2$
$S_{C_2H_6} = \frac{3}{2} k_1 [M]^2$
$S_{C_2H_2} = k_1 [M]^2$
$S_{M_{total}} = -(k_I[A] + k_p\lambda_0 + k_{trm}\lambda_0)[M] - \left(\frac{5}{2}k_1 + \frac{k_6}{2} \sqrt{\frac{2k_1}{k_t}} [M]^2\right)$
$S_{T_{total}} = -\Delta H(-k_I[A][M] - k_p\lambda_0[M] - k_{trm}\lambda_0[M]) - \Delta H_{decomp} \left(3k_1 + k_6 \sqrt{\frac{2k_1}{k_t}}\right) [M]^2$

3.4 Investigating the effects of the operating parameters

The effects of operating parameters on the temperature distribution including the inlet initiator mass fraction and the inlet temperature are studied. The values of operating parameters are shown in Table 9.

Table 9 The values of operating parameters

Parameters	Values	Units
Inlet initiator mass fraction	1.2×10^{-5} , 1.2×10^{-4} , 1.2×10^{-3}	Dimensionless
Inlet temperature	400, 460, 510	K

4. Results and Discussions

Firstly, the 3D CFD model of the autoclave polymerization reactor for LDPE production was developed by taking into account the polymerization reaction. The simulation results were then validated with the literature data from Zhou et al. (2001) at the same operating condition as shown in Figure 2. It was found that the simulation results agreed well with the literature data. The percentage difference between the simulation result and the literature data was less than 1%.

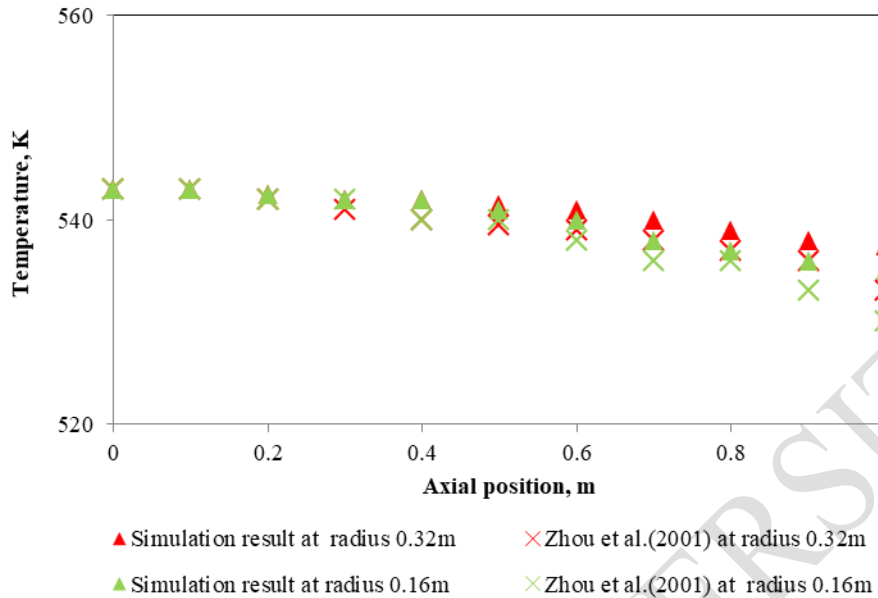


Figure 2 Axial distributions of temperature in the autoclave reactor at different radial positions

The temperature in the autoclave reactor could indicate the runaway phenomena, so this model was brought to simulate within both polymerization and decomposition reactions. High temperature in the reactor was affected by the inlet initiator mass fraction and inlet temperature. The inlet initiator mass fraction was one of the important operating parameter affecting the runaway phenomena. Figure 3 showed the temperature profile in the autoclave reactor at different values of the inlet initiator mass fraction. It was found that the temperature in the reactor increased as the initiator mass fraction increased. The runaway phenomena took place at very high mass fraction of initiator as shown in Figure 3(c).

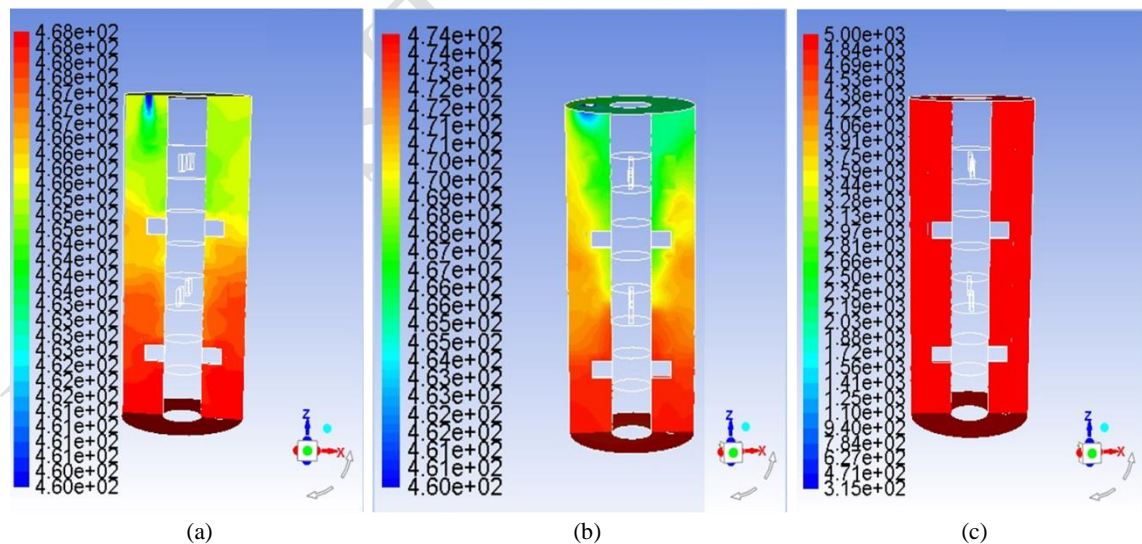


Figure 3 Temperature distributions (K) at different values of the inlet initiator mass fraction: (a) 1.2×10^{-5} (b) 1.2×10^{-4} and (c) 1.2×10^{-3}

The inlet temperature was another important parameter affecting the temperature distribution. Figure 4 showed the temperature profile in the autoclave reactor at different values of the inlet temperature.

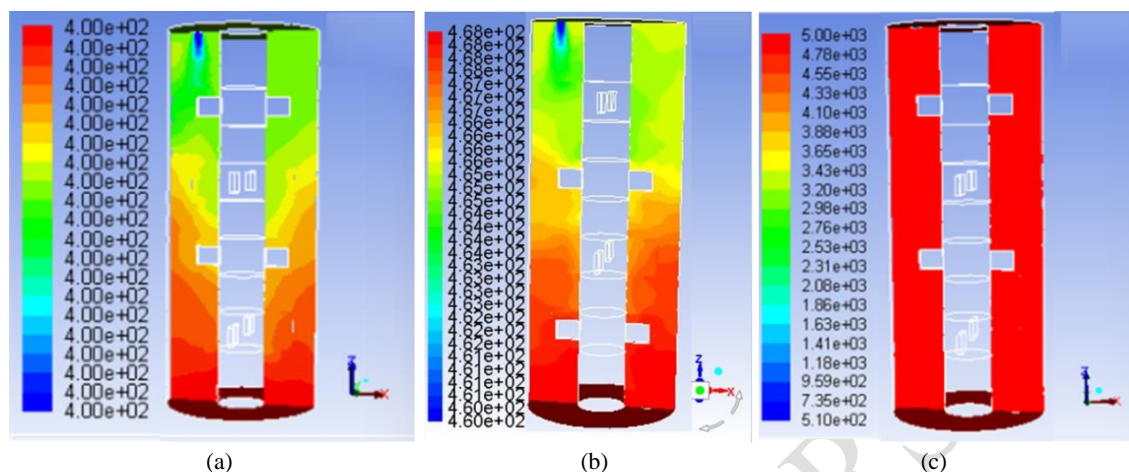


Figure 4 Temperature distributions (K) at different values of the inlet temperature:
(a) 400 K (b) 460 K and (c) 510 K

The runaway phenomena took place at too high inlet temperature. As shown in Figure 4(c), the values of temperature in the autoclave reactor rose up to 5,000 K due to the large amount of heat produced from the decomposition of ethylene.

5. Conclusion

In this paper, a CFD model of an autoclave polymerization reactor for LDPE production was developed. The effects of the inlet initiator mass fraction and the inlet temperature on temperature distribution were studied. The rapidly increasing temperature came from the decomposition of ethylene. The simulation results showed that the runaway phenomena took place at the inlet initiator mass fraction and the inlet temperature of 1.2×10^{-3} and 510 K, respectively.

6. Acknowledgements

This project was supported by Mahidol University.

7. References

- Ham, J. Y., & Rhee, H. K. (1996). Modeling and control of an LDPE autoclave reactor. *Journal of Process Control*, 6(4), 241-246.
- Kolhapure, N. H., Fox, R. O., Daiss, A., & Mahling, F. O. (2005). PDF simulations of ethylene decomposition in tubular LDPE reactors. *American Institute of Chemical Engineers Journal*, 51, 585-606.
- Pladis, P., & Kiparissides, C. (1999). Dynamic modeling of multizone multifeed high-pressure LDPE autoclaves. *Journal of Applied Polymer Science*, 73, 2327-2348.
- Read, N. K., Zhang, S. X., & Ray, W. H. (1997). Simulations of a LDPE reactor using computational fluid dynamics. *American Institute of Chemical Engineers Journal*, 43, 104-117.
- Tosun, G., & Bakker, A. (1997). A study of macrosegregation in low-density polyethylene autoclave reactors by computational fluid dynamic modeling. *Industrial and Engineering Chemistry Research*, 36, 296-305.
- Villa, C. M., Dihora, J. O., & Ray, W. H. (1998). Effects of imperfect mixing on low-density polyethylene reactor dynamics. *American Institute of Chemical Engineers Journal*, 44(7), 1646-1656.

- Zhang, S. X., Read, N. K., & Ray, W. H. (1996). Runaway phenomena in low-density polyethylene autoclave reactors. *American Institute of Chemical Engineers Journal*, 42(10), 2911-2925.
- Zheng, H., Huang, H., Liao, Z., Wang, J., Yang, Y., & Wang Y. (2014). Computational fluid dynamics simulations and experimental validation of macromixing and flow characteristics in low-density polyethylene autoclave reactors. *Industrial and Engineering Chemistry Research*, 53(38), 14865-14875.
- Zhou, W., Marshall, E. & Oshinowo, L. (2001). Modeling LDPE tubular and autoclave reactors. *Industrial and Engineering Chemistry Research*, 40(23), 5533-5542.

RANGSIT UNIVERSITY